

A NUMERICAL ANALYSIS FOR VISCOUS FLUID FLOW BY USING DIFFERENTIAL EQUATION IN COMPUTATIONAL FLUID DYNAMICS

G. Chandra Mohan

Asst. professor

Department of H&S

St. Martins engineering college

Chandumohan2006@gmail.com

Ch. Anusha

Asst. professor

Department of H&S

Mallareddy college of engineering for

women

chalamalasettianu@gmail.com

Abstract:

Rather high computing cost is required for the introduction of artificial dissipation into the method for a direct numerical solution (DNS) or a certain restricting technique even though algorithms in simulation-based studies are becoming a big part of the liquid flow analyses. Viscous fluids are computation by using finite element methods numerical equations plays an important role in the preparation of fluid dynamics.

Numerical equation simulations have the positive advantage in addressing comparative analyzes using measured dynamics; the latest research focuses on improving the viscous fluid differential equation process. In this study, we present an overall method for the resolution of fluid mechanic problems without any device of stabilization or fracturing. Its generalization to applications of multiple physics is therefore simple. We discuss new numerical problems and rigorously explain the approach.

Key words- Numerical studies, Differential equations, Fluid dynamics

1.0 Introduction

It illustrates the creation of non-Newtonian energy equations and the formulation of conservation equations in advanced coordinate systems, and the introduction of diverse body forces into dynamic equations. This will raising complicated computational pressures in the resolution of fluid dynamic equations. Their synchronization schemes include the Cartesian, cylindrical and sphere fields, and are supported by continuity, navier storages and the energization equations.

The guideline is based on Newton's Laws and Reynold's theorem of transport[1,2] fundamental concepts, which can be represented in general as an integral equation. However, such a general form is not convenient for the precise analysis down to the scale of fluid element parcels [3]. Therefore, the Eulerian method takes the phase and expands further into varying types of tensor and indicial notation equations for spatial descriptors and flux fields. Continuum mechanics and procedural rules are being introduced[4,5]. Continuity equation can be used as a nonlinear equation of diffusion with the normal drift concept and encourages all-around applications in many fields such as cross-modeling [6], aircraft debris cloud evolution [7], biomedical imaging [8] and curve analyzes [9]. This can also be regarded as an initial boundary issue[10] or as a question of cauchy[11].

2.0 Fluid flow equations

Isothermal flow of viscous fluid is modelled in Cartesian coordinates by using the balance equations of mass and linear momentum:

$$\frac{\partial \rho}{\partial t} + \frac{\partial v_i \rho}{\partial x_i} = 0 ,$$

$$\frac{\partial \rho v_j}{\partial t} + \frac{\partial}{\partial x_i} (v_i \rho v_j - \sigma_{ij}) = \rho g_j .$$

respectively, where ρ denotes the mass density, v_i the velocity, σ_{ij} the non-convective flux term

(Cauchy's stress), g_i specific provision (gravity); here and now we extend the Summation Convention of Einstein to repeated indicators. A linear stress relation provides sufficient precision in the case of Newtonian fluids, such as water, oil or alcohol. This linear relation is sometimes called the Navier–Stokes equation:

$$\sigma_{ij} = (-p + \lambda d_{kk})\delta_{ij} + 2\mu d_{ij} , \quad d_{ij} = \frac{1}{2} \left(\frac{\partial v_i}{\partial x_j} + \frac{\partial v_j}{\partial x_i} \right)$$

The substance constants were λ, μ ; and a new (hydrostatic) pressure parameter was called p . The law of motion in literature is often referred to as the Navier – Stokes equation, i.e. the substance equation introduced into the equilibrium equation.

$$\frac{\partial v_i}{\partial x_i} = 0 ,$$

The above mentioned equations are accomplished locally in analytical mechanics (either at any infinite volume variable or simply pointing in space). For a measure, we distinguish the space by using the form of the finite element (FEM). The theoretical functions of the unknown virgins v_i and p are seen within each element by shape functions, i.e. by means of a distinct entity. The functions of form are not smooth, they are C_n with a n finite.

We use one balance equation for calculating the pressure and another balance equation for calculating the velocity. This must be remembered that the two balancing equations are combined and that the measurement pressure and velocity are not precisely specified. It is appropriate to remember the balance equations. This technique is already followed in Chorin's system and then widely used by stresses controlled by the Petrov – Galerkin process (PSPG). More powerful numerical approaches are using all equilibrium equations for the two unknowns.

3.0 Variational Formulation

Consider the following general balance equation:

$$\left(\int_{\Omega} \psi \, dv \right)' = \int_{\Omega} z \, dv + \int_{\partial\Omega} (f + \phi) \, da$$

Table 1. Volume densities, their supply and flux terms in the balance equations.

ψ	z	f	ϕ
ρ	0	$n_i(w_i - v_i)\rho$	0
ρv_j	ρg_j	$n_i(w_i - v_i)\rho v_j$	σ_{ij}
$\rho(s_j + \epsilon_{jkl}x_k v_l)$	$\rho(\ell_j + \epsilon_{jkl}x_k g_l)$	$n_i(w_i - v_i)\rho(s_j + \epsilon_{jkl}x_k v_l)$	$m_{ij} + \epsilon_{jkl}x_k \sigma_{il}$

Without influencing the underlying Physics, the domain speed can be random chosen. Here we set $w_i = 0$ to correct the domain. We assume the rests of the gas, $v_i(x, t = 0)$, are initially 0, and are of a homogenous material, $r(x, t = 0) = \text{const}$. In addition, we assume that the flow is unstable, i.e. the mass density stays stable at $\dot{\rho} / \dot{\Omega} = 0$. After using the theorem Gauss-Ostrogradskiy, we obtain

$$\int_{\Omega} \rho \frac{\partial v_i}{\partial x_i} dv = 0,$$

$$\int_{\Omega} \left(\rho \frac{\partial v_j}{\partial t} - \rho g_j + \rho \frac{\partial v_i v_j}{\partial x_i} - \frac{\partial \sigma_{ij}}{\partial x_i} \right) dv = 0,$$

$$\int_{\Omega} \left(\rho \frac{\partial s_j}{\partial t} + \rho \epsilon_{jkl} x_k \frac{\partial v_l}{\partial t} - \rho \ell_j - \rho \epsilon_{jki} x_k g_i - \frac{\partial}{\partial x_i} (-v_i \rho (s_j + \epsilon_{jkl} x_k v_l) + m_{ij} + \epsilon_{jkl} x_k \sigma_{il}) \right) dv = 0.$$

Where the density, s_i , its flux (paired stress) term, m_{ij} , and the term 'i' of its supply all vanish for a non-polar medium like water (symmetric stress supply). The angle momentum is then the same as the momentum (linear)

$$\int_{\Omega} \epsilon_{jkl} x_k \left(\rho \frac{\partial v_l}{\partial t} - \rho g_l + \rho \frac{\partial v_i v_l}{\partial x_i} - \frac{\partial \sigma_{il}}{\partial x_i} \right) dv = 0,$$

$$\int_{\Omega} \left(\rho \frac{\partial v_l}{\partial t} - \rho g_l + \rho \frac{\partial v_i v_l}{\partial x_i} - \frac{\partial \sigma_{il}}{\partial x_i} \right) dv = 0,$$

We continue using the discrete representations of continuous fields; but we skip a clear difference in the notation, because we never merge continuous and discrete functions. We emphasize that it is necessary to select the scalar testing function and suggest that

$$\int_{\Omega} \rho \frac{\partial v_i}{\partial x_i} \delta p dv = 0,$$

$$\int_{\Omega} \left(\rho \frac{\partial v_j}{\partial t} - \rho g_j + \rho \frac{\partial v_i v_j}{\partial x_i} - \frac{\partial \sigma_{ij}}{\partial x_i} \right) \delta v_j dv = 0,$$

$$\int_{\Omega} \left(\rho \frac{\partial v_j}{\partial t} - \rho g_j + \rho \frac{\partial v_i v_j}{\partial x_i} - \frac{\partial \sigma_{ij}}{\partial x_i} \right) \frac{\partial \delta p}{\partial x_j} dv = 0.$$

4.0 Algorithm and Computation

For all applications, continuous finite elements are used. In 3D we use tetrahedrons as elements and in 2D we use triangles as elements — with both linear-form functions, i.e. grade $n = 1$ defining functions. The primitive variables are pressure and velocity; they are represented with corresponding nodal values interpolated using the form functions. Concretely, 4 primitive variables $\mathbf{P} = \{p, v_1, v_2, v_3\}$ in three-dimensional space belong to

$$\mathcal{V} = \{ \mathbf{P} \in [\mathcal{H}^n(\Omega)]^4 : \mathbf{P}|_{\partial\Omega} = \text{given} \}$$

The functional Form = $F(\mathbf{P}, \Delta\mathbf{P})$ is an integral of the function depending on the primitive variables \mathbf{P} and their variations (test functions) $\Delta\mathbf{P}$. We know the correct values of \mathbf{P} at $t = 0$. The weak form is initially zero—we obtained it by subtracting left-hand sides from right-hand sides in the balance equations. We search for $\mathbf{P}(t + Dt)$ at the next time step, $Dt + t$, by

using the known values $\mathbf{P}(t)$. By rewriting the unknowns $\mathbf{P}(t + \Delta t)$ in terms of the known values

$$P(t + \Delta t) = P(t) + \Delta P(t)$$

$$F(P + \Delta P, \delta P) = F(P, \delta P) + \nabla_p F(P, \delta P) \cdot \Delta P$$

$$\nabla_p F(P, \delta P) \cdot \Delta P = \lim_{\epsilon \rightarrow 0} \frac{d}{d\epsilon} F(P + \epsilon \Delta P, \delta P)$$

5.0 Comparative Analysis

This study is important to demonstrate the monotonous local convergence which is the main and prominent feature of the FEM. For a flow problem, the precision is improved by reducing mesh size at every level. Second, we pose two-dimensional benchmarking problems to validate the method's robustness.

Consider a laminar flow in an infinite pipe as a result of the given pressure difference.

This structure is the Hagen – Poiseuille flow with an observation that the fluid is on the pipe only, and has a static solution obtained in cylindrical co-ordinates r , θ , z . r . The tubes are z -oriented, set as the pipe axis. State with no break, $v_i = 0$ is added to the exterior walls, $r = a$.

The Stability Solution

$$v_i = \begin{pmatrix} 0 \\ 0 \\ -\frac{dp}{dz} \frac{a^2}{4\mu} \left(1 - \frac{r^2}{a^2}\right) \end{pmatrix}$$

for a continuous viscous fluid incompressible flow like viscosity μ vapor. For a study of consistency and exactitude, we use this approach. A 3D length pipe is built, the pressure being supplied in the inlet and outlet as the Dirichlet line, $p(z = 0) = p_{in}$ and $p(z = \mu) = p_{out} = p_{out}$.

The flow is driven by the disparity in pressure, which neglects the gravity. In fact, we want the constant state in which the inertia concept disappears. We also set radial and circumferential speeds to nil on the entrance and exit to mimic the infinite wire. FEM computation is realized in Cartesian coordinates, so we basically allow v_z on inflow plane, $x = 0$, and outflow plane, $x = \mu$, by setting $v_x = v_y = 0$ as Dirichlet conditions.

The pressure distribution is expected to be linear along z , hence, for the analytical solution $dp/dz = (p_{out} - p_{in})/\mu$, the characteristic velocity for calculating the Reynolds number:

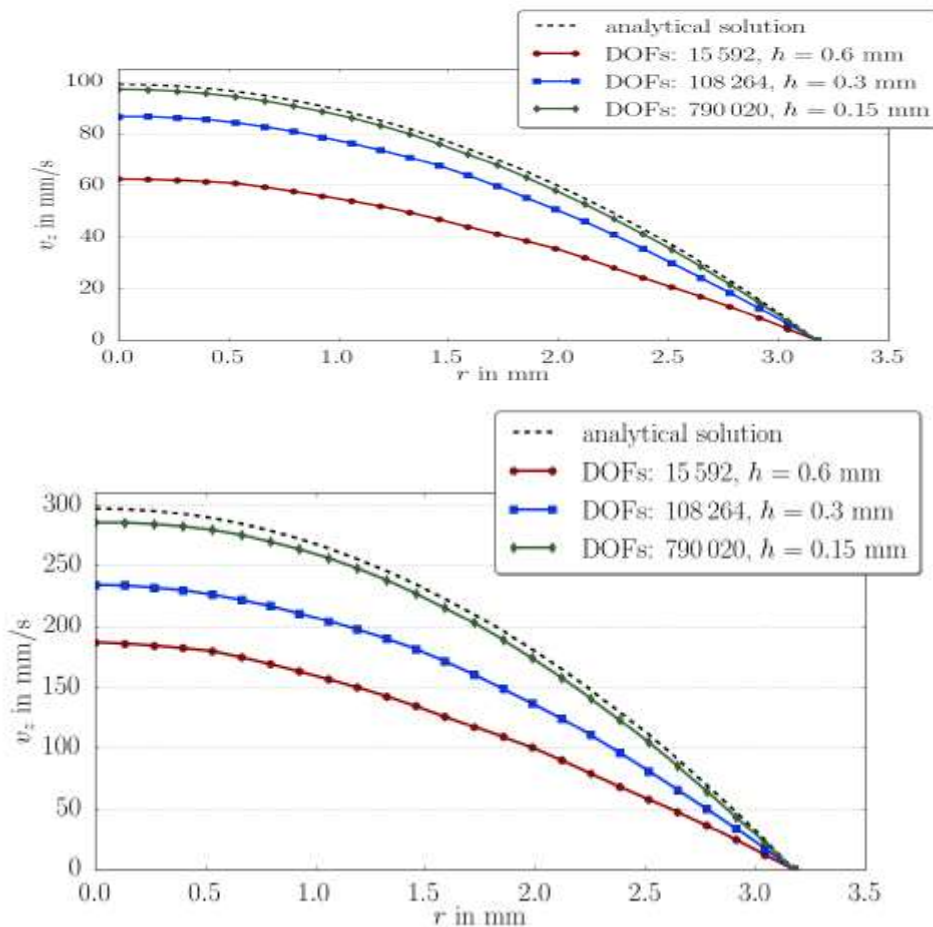
$$Re = \frac{v_z^M D \rho}{2\mu}$$

5.1 Problem solvation

We create the mesh with a global product length h for a narrow pipeline of one inch and one quarter inch wide. The SI units we use are $25 \text{ mm} = 25,4 \text{ mm}$, $D = 6,35 \text{ mm}$, and the fluid of water

$$\rho = 998.2 \times 10^{-6} \text{ g/mm}^3, \quad \mu = 1001.6 \times 10^{-6} \text{ Pas}, \quad \lambda = 0.6 \text{ Pas}.$$

Three separate meshes beginning from a global band length tetrahedron, $h=0.6$ mm, then reduced by half, are measured using a typical convergence model. A new mesh is produced for each simulation, so that the number of nodes in 3D does not increase by 23 specifically. The mesh efficiency is almost similar due to the use of the same algorithm for the relatively simple geometry. As shown in figure 1 for 2 separate Reynold numbers, the expected monotonic convergence was achieved.



It is appropriate to emphasize two important facts. First, even a thin mesh means that the velocity is parabolized along the diameter. Second, at $R = 0$ with small Reynolds the relative error is 1.1 percent.

It is appropriate to emphasize two important facts. First, even a thin mesh means that the velocity is parabolized along the diameter. Second, at $R = 0$ with small Reynolds the relative error is 1.1 percent.

Using SciPy sets, for Bessel functions and its roots, to use (semi-)analytical approach, and then choose $N = 50$. By selecting a best mesh, namely a mesh of $h = 0.15$ mm, resulting from the convergence analysis in the steady-state case, we can measure the solution on time by using various time measures. In Figure 2 we show the maximum value $v_z (r = 0, t)$ for

different time levels, which shows the predicted convergence, . time steps and distribution at different time instants for the smallest time step.

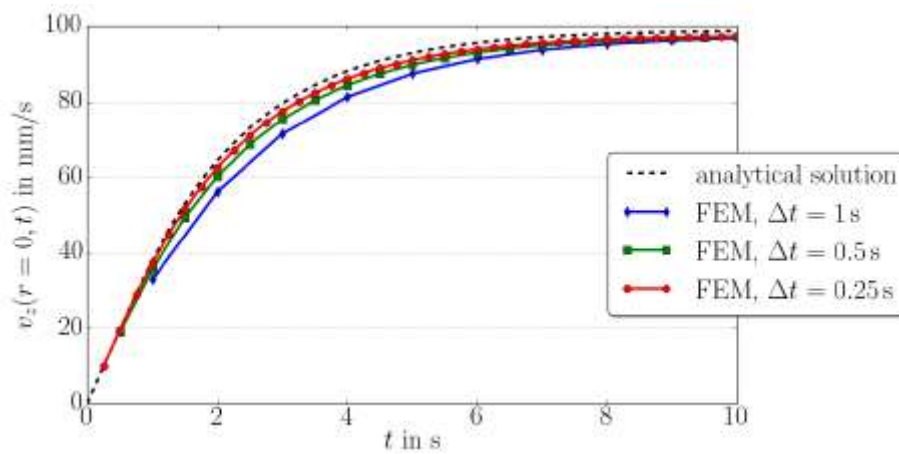


Figure 2. Three-dimensional computation of transient solution and its comparison to the analytical solution in a pipe for $Re = 313$ in (a) $\Delta t = 1, 0.5, 0.25$ s; (b) $\Delta t = 0.25$ s.

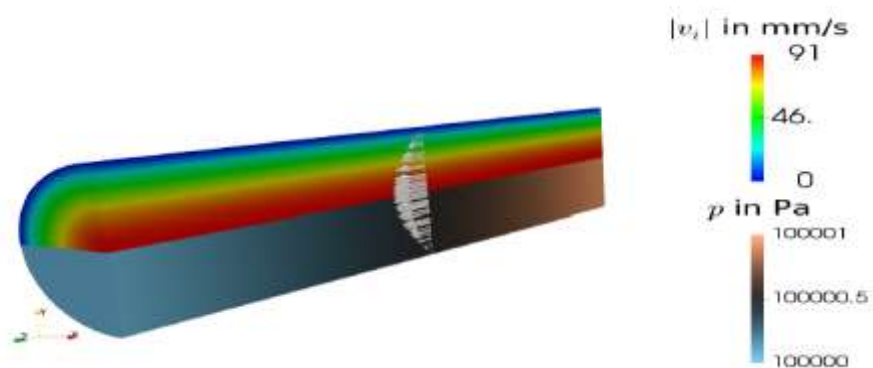
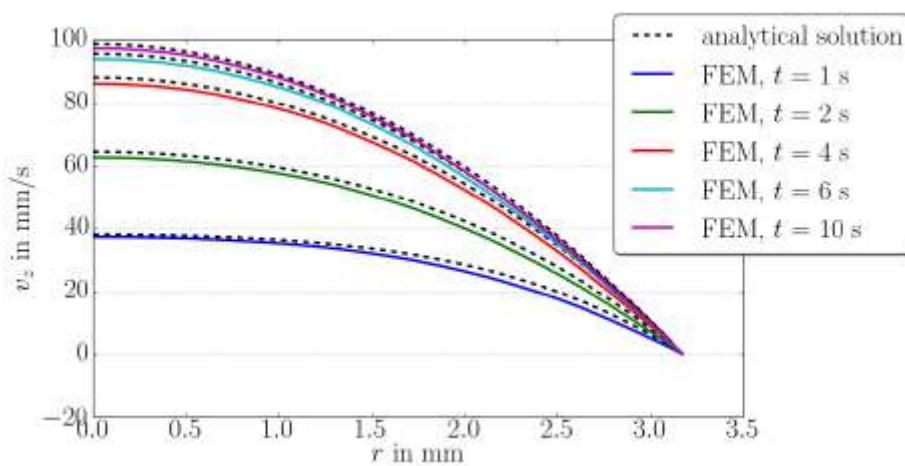


Figure 3 shows the transient pipe flow at $t = 5$ s, shown on the half of the pipe (upper part: velocity and lower part: pressure) for $Re = 313$.

Results from the reference solution and results obtained by the proposed method show no

significant difference up to $Re = 5000$. This good agreement fails to be the case in the higher Reynolds number.

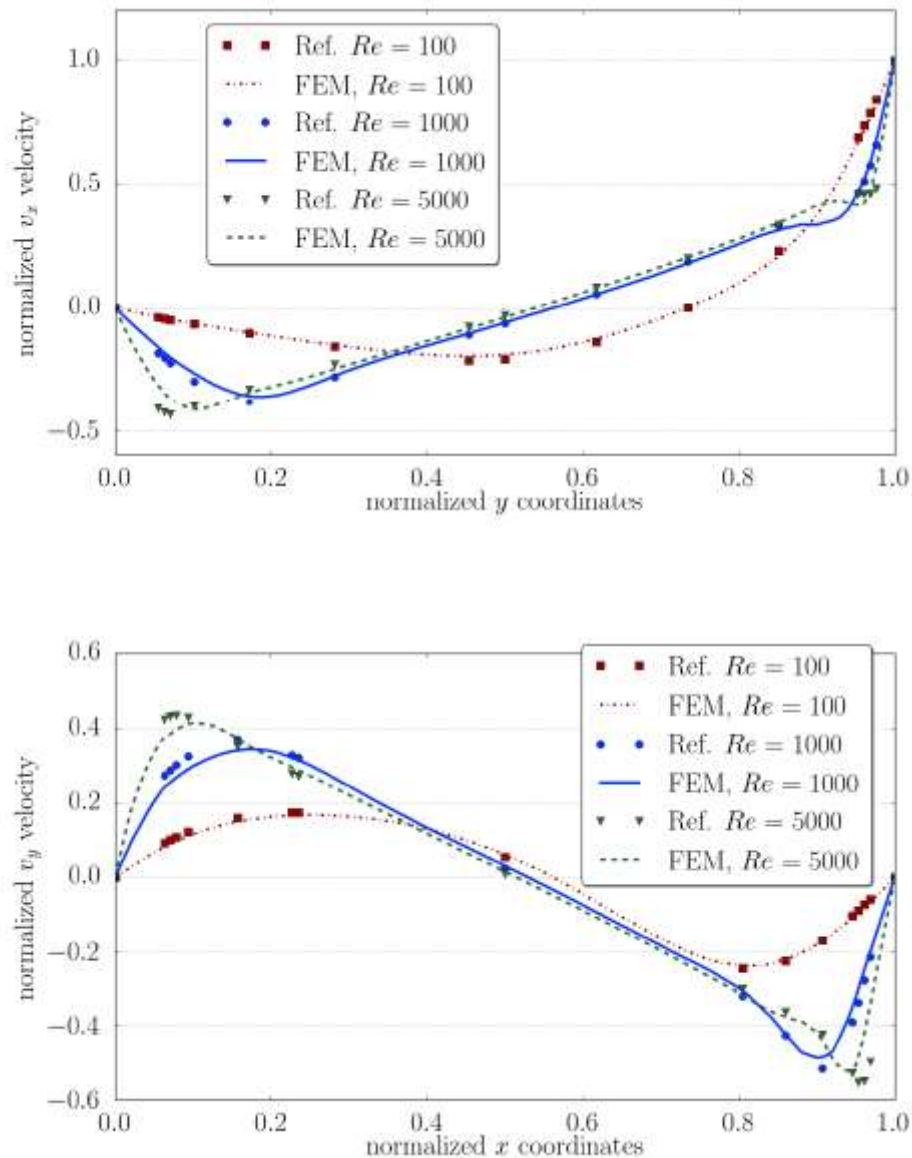


Figure 4: Velocity distribution in the lid driven cavity benchmark problem. (a) Horizontal velocities along the vertical axis through the center are divided by the (given) lid velocity. (b) Vertical velocities along horizontal axis through the center are normalized by the lid velocity. For three different Reynolds numbers, the results are compared to the reference solution

6.0 Conclusions

Convergence in space and time is difficult to achieve in FEM for flow problems. The accuracy is only possible by using extremely high degrees of freedom. With the proposed method, attained a good accuracy with relatively coarse meshes. Local monotonic convergence in space and time is a remarkable quality of the FEM and our method exploits this feature. This property is of paramount importance for problems where the accurate solution is not known. Based on the local monotonic convergence, a posteriori error analysis is possible. Hence, the proposed method is reliable.

7.0 References

- [1] Sultanian, B.K. "Control Volume Analysis." In: Sultanian, B.K. *Fluid mechanics: An Intermediate Approach*. CRC Press, 2016.
- [2] Emanuel, G. "Conservative Equations." In: Emanuel, G. *Analytical Fluid Dynamics*. CRC Press, 2016.
- [3] Graelbel W.P. *Advanced Fluid Mechanics*. Elsevier, 2007.
- [4] Moore, R.L. "Foundations of point set theory." *American Mathematical Society Colloquium Publication 13* (1962).
- [5] Charatonik, J.J. *History of Continuum Theory*. Kluwer Academic Publisher, 1998.
- [6] Carlier, G. and Laborde, M. "Remarks on continuity equations with nonlinear diffusion and nonlocal drifts." *Journal of Mathematical Analysis and Applications* 444 (2016): 1690-1702.
- [7] Letizia, F., Colombo, C. and Lewis, H.G. "Multidimensional extension of the continuity equation method for debris clouds evolution." *Advances in Space Research* 57 (2016): 1624-1640.
- [8] Dawood, M., Brune, C., Jiang, X., Buther, F., Burger, M., Schober, O., Schafers, M. and Schafers, K.P. *A continuity equation based optical flow method for cardiac motion correction in 3D PET data. Medical Imaging and Augmented Reality, Lecture Notes in Computer Science*, 2010.
- [9] Stepanov, E. and Trevisan, D. "Three superposition principles: Currents, continuity equations and curves of measurement." *Journal of Functional Analysis* 272 (2017): 1044-1103.
- [10] Crippa, G., Donadello, C. and Spinolo, L.V. "Initial boundary value problems for continuity equations with BV coefficients." *Journal of Mathematiques Pures et Appliquees* 102 (2014): 79-98.
- [11] Bogacheva, V.I., DaPrato, G., Röckner, M. and Shaposhnikova, S.V. "On the uniqueness of solutions to continuity equations." *Journal of Differential Equations* 259 (2015): 3854-3873.
- [12] Lee, H. and Xu, S. "Fully discrete error estimation for a quasi-Newtonian fluid–structure interaction problem." *Computers and Mathematics with Applications* 71 (2016): 2373-2388.
- [13] Bilen Emek Abali "An Accurate Finite Element Method for the Numerical Solution of Isothermal and Incompressible Flow of Viscous Fluid" *Fluids* 2019, 4, 5; www.mdpi.com/journal/fluids
- [14] Lee, M.; Moser, R.D. Direct numerical simulation of turbulent channel flow up to $Re = 5200$. *J. Fluid Mech.* **2015**, 774, 395–415.